

Electronic Supplementary Information

Robust Redox-Active Hydrogen-Bonded Organic Framework for Rechargeable Batteries

Xiaolin Liu,^{†a} Xiya Yang,^{†a} Hailong Wang,^{*a} Ichiro Hisaki,^{*b} Kang Wang and Jianzhuang Jiang^{*a}

^a. Beijing Advanced Innovation Center for Materials Genome Engineering, Beijing Key Laboratory for Science and Application of Functional Molecular and Crystalline Materials, Department of Chemistry and Chemical Engineering, School of Chemistry and Biological Engineering, University of Science and Technology Beijing, Beijing 100083.

^b. Division of Chemistry, Graduate School of Engineering Science, Osaka University, 1-3 Machikaneyama, Toyonaka, Osaka 560-8531, Japan.

E-mail: Email: hlwang@ustb.edu.cn (H.W.), hisaki@chem.es.osaka-u.ac.jp (I.H.) and jianzhuang@ustb.edu.cn (J.J.)

[†] These authors contributed equally to this work.

Caption of Content

Experimental section	S2
Figure S1. Cycling performance of CPHATN-1a at 0.1 C	S5
Figure S2. PXRD pattern of as-synthesized HOF (CPHATN-1)	S5
Figure S3. The ex-situ XRD pattern of CPHATN-1a-based electrode at the selected states.....	S6
Figure S4. Rietveld refinements of the PXRD pattern data.....	S6
Figure S5. The SEM images of cathodes after different cycles.....	S7
Table S1. The fitting errors of the simulated equivalent circuit of CPHATN-1a	S8
Table S2. Performance metrics of representative organic frameworks as cathode materials for LIBs	S8

I. Experimental section.

General information. All chemicals were obtained from commercial sources and used without further purification. The organic building block, hexaazatrinaphthylene derivative with carboxyphenyl groups (CPHATN), was synthesized according to the procedure listed in previous reference.^[S1]

Synthesis of CPHATN-1. The crystallization of CPHATN to give light yellow crystals (CPHATN-1) was synthesized according to the procedure listed in previous reference.^[S1]

By evaporation of a mixed solution of N-methylpyrrolidone (NMP)] and 1,2,4-trichlorobenzene (TCB)] at 333 K for 12 h allowed formation of a block-shaped P-1 crystal [CPHATN-1(TCB)], which has a layered structure of H-HexNet frameworks.

Activation of CPHATN-1(TCB) was accomplished by heating at 463 K for 72 h under vacuum conditions, giving the corresponding desolvated material CPHATN-1a possessing permanent porosity.

Physical characterization. NMR spectra were recorded on a Bruker DPX 400 spectrometer (^1H : 400 MHz, ^{13}C : 100 MHz). ^1H NMR spectra were referenced internally using the residual solvent resonances ($\delta = 7.26$ ppm for CDCl_3 , $\delta = 2.50$ ppm for $\text{DMSO-}d_6$) relative to SiMe_4 . ^{13}C NMR spectrum was referenced internally by using the solvent resonance ($\delta = 77.00$ ppm for CDCl_3 , $\delta = 39.50$ ppm for $\text{DMSO-}d_6$). Powder X-ray diffraction (PXRD) was collected at room temperature on a PANalytical Empyrean series 3 diffractometer equipped with $\text{Cu K}\alpha$ radiation operating at 45 kV and 40 mA and on a diffracted-beam graphite monochromator. Before the gas sorption measurements, as-synthesized crystals were evacuated to 6 μmmHg at 463 K to generate activated samples. The gas sorption isotherms were measured on a Micromeritics ASAP 2020 surface area analyzer, and the measurement temperature was maintained at 77 K with a liquid nitrogen bath. X-ray photoelectron spectroscopy (XPS) data were conducted on an Thermo Scientific K-Alpha⁺ system. Mono Al $\text{K}\alpha$ X-ray (15 mA \times 15 KV) was utilized as the irradiation source. All measurements were performed in the CAE mode with the reference of C 1s (284.8 eV). Scanning electron microscope (SEM) measurements were performed on HITACHI SU8010 microscope operated at an accelerating voltage of 3.0 KV.

Investigation of the performance of CPHATN-1a as cathode for lithium-ion battery. *Electrochemical performance* was collected in CR2032-type coin cells, which were assembled in an argon-filled glove box with H₂O and O₂ level <0.1 ppm. To prepare the working electrodes, viscous slurry was first prepared by mixing active materials (CPHATN-1a) with carbon black (Super-P) and polyvinylidene fluoride (PVDF) in a weight ratio of 50:40:10. N-Methylpyrrolidone (NMP) was used as the solvent. Then the slurry was pasted onto Al foil. The electrode film was punched into small disks with diameter of 10 mm. Li foil was used as the counter electrode and Celgard 2400 as the separator. The electrolyte is 1M lithium bis(trifluoromethanesulfonyl)imide (LiTFSI) in 1,3-dioxolane and dimethoxyethane=1:1 vol%. The cycling performance of the cells was tested on LAND CT2001A battery system at various current densities within voltage range of 1.2-4.0 V (vs Li/Li⁺). The specific capacity is calculated based on the mass of the active material (CPHATN-1a). The CV measurements were performed on CHI660E electrochemical workstation. The EIS were conducted at a 5 mV ac oscillation amplitude over frequency range of 100kHz-1 Hz. The theoretical capacity of CPHATN-1a as cathode for lithium-ion battery was calculated by Faraday's law:

$$Q_{CPHATN-1a} = \frac{nF}{3.6M_w}$$

during which n is the number of charge carrier (For repeat unit of CPHATN-1a, n=6); F is the Faraday constant; M_w is the molecular weight of the active material (for repeat unit of CPHATN-1a, M_w=1104.2).

II. Characterization and properties.

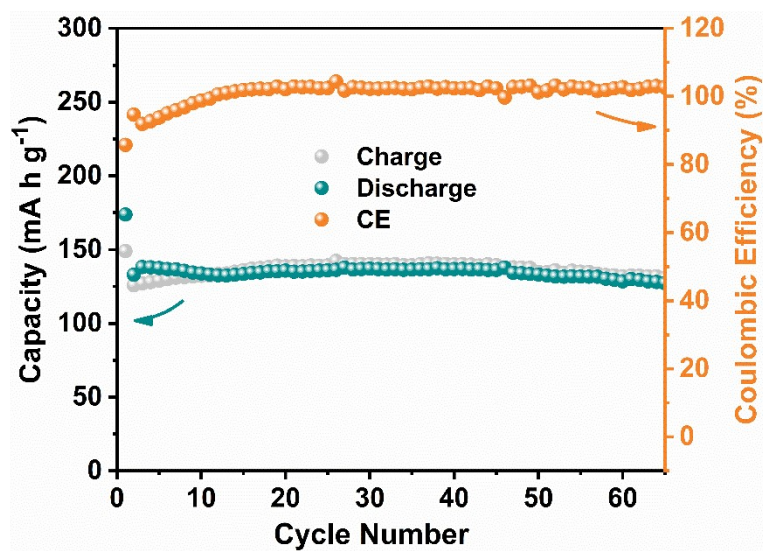


Figure S1. Cycling performance of CPHATN-1a at 0.1 C.

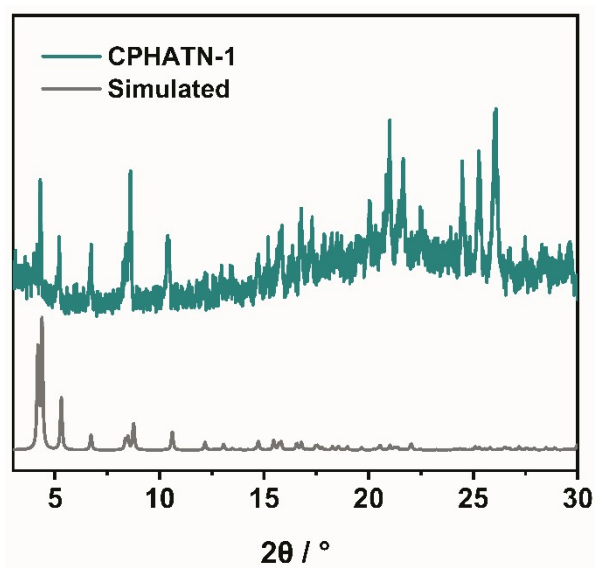


Figure S2. PXRD pattern of as-synthesized HOF (CPHATN-1).

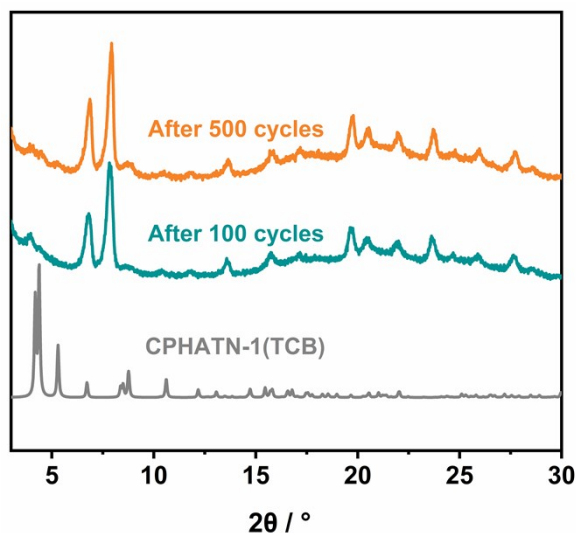


Figure S3. The ex-situ XRD pattern of CPHATN-1a-based electrode at the selected states.

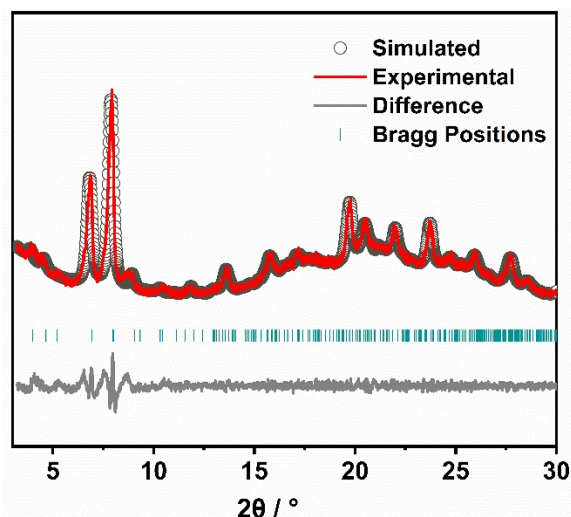


Figure S4. Rietveld refinements of the PXRD pattern data: Experimental (red), calculated (circles), and difference (line below observed and calculated patterns) and vertical bars indicate the calculated positions of Bragg peaks. $GOF = 1.10$, $R_p = 0.42\%$, $R_{wp} = 0.63\%$.

The agreement between experiment and simulation is very well. In the structural model after cycling stability test, the lattice parameters were obtained from indexing the experimental PXRD pattern. The results show that the CPHATN-1 crystal structure remains essentially the same upon cycling stability test, in terms of crystal symmetry and framework arrangement. However, the unit cell parameters do change a bit: After

cycling stability test (from PXRD data: $a = 7.1733 \text{ \AA}$, $b = 19.6491 \text{ \AA}$, $c = 22.9524 \text{ \AA}$, $\alpha = 73.829$, $\beta = 89.764$, $\gamma = 86.830$). This corresponds to the slight movement of the 001, 010 and 011 crystal planes.

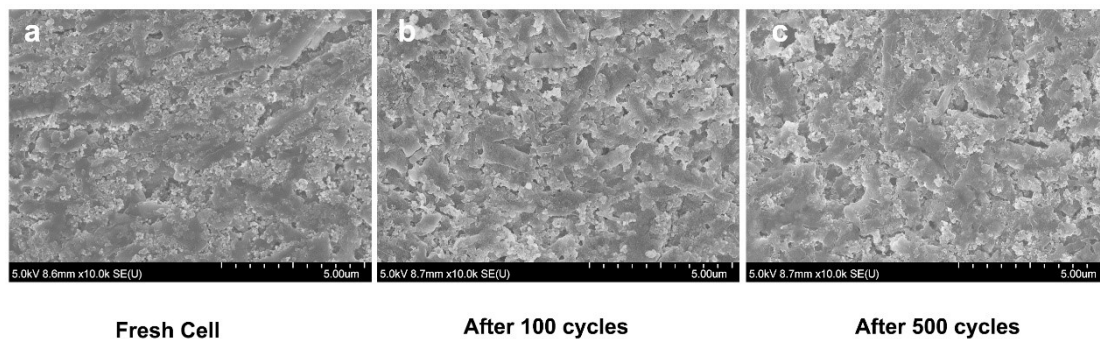
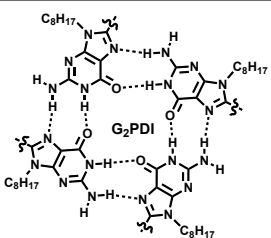
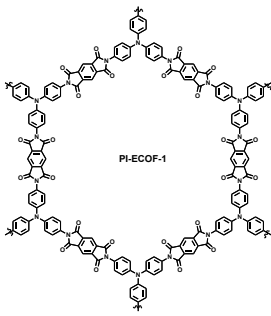
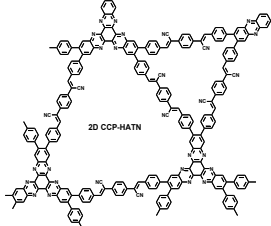


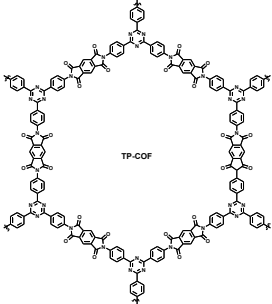
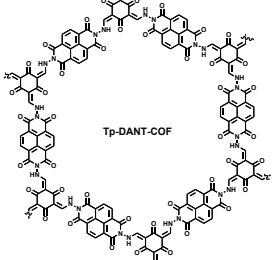
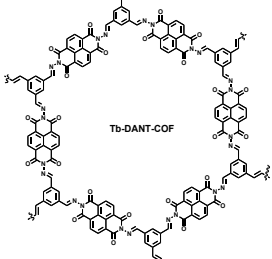
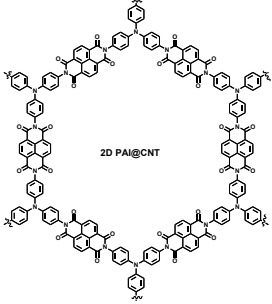
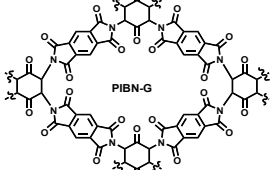
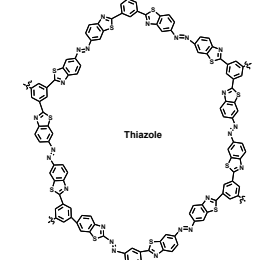
Figure S5. The SEM images of cathodes after different cycles. (Current density: 1 C)

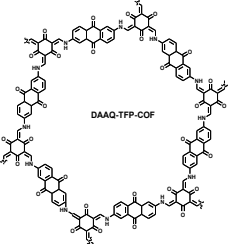
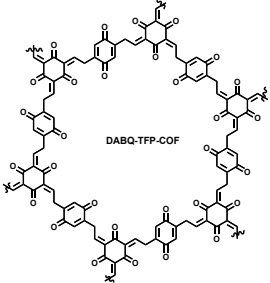
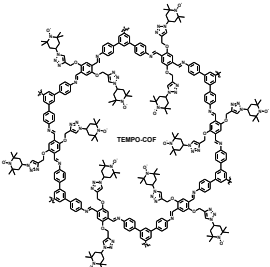
Table S1 The fitting errors of the simulated equivalent circuit of CPHATN-1a.

	R_c (Ω)	R_f (Ω)	R_{ct} (Ω)	Sum (Ω)
CPHATN-1a	2.13	6.84	16.01	24.98
Fitting Error (%)	2.31	13.7	5.8	-

Table S2. Performance metrics of representative organic frameworks as cathode materials for lithium-ion batteries.

Structure	Theoretical Capacity (mA h g^{-1})	Practical Capacity (mA h g^{-1})	Potential (V)	Cycling number	Ref.
CPHATN-1a	145	128	1.2-4 V	500	This work
	37.5	27	1.5-3 V	300	[S2]
	142	112	1.5 V-3.5 V	300	[S3]
	117	116	1.2-3.9 V	1000	[S4]

 <p>TP-COF</p>	256	110	1.5-3.5 V	500	[S5]
 <p>Tp-DANT-COF</p>	134	94	1.5-4.0 V	200	[S6]
 <p>Tb-DANT-COF</p>	145.7	123.7	1.5-4.0 V	100	[S6]
 <p>2D PAI@CNT</p>	125.9	104.4	1.5-3.5 V	8000	[S7]
 <p>PIBN-G</p>	280	271	1.5-3.5 V	300	[S8]
 <p>Thiazole</p>	145	140	1.0-3.0 V	1000	[S9]

 <p>DAAQ-TFP-COF</p>	151	145	1.5-4 V	1800	[S10]
 <p>DABQ-TFP-COF</p>	221	210	1.5-4 V	/	[S10]
 <p>TEMPO-COF</p>	129	115	1.5-4 V	/	[S10]

Reference

- [S1] I. Hisaki, Y. Suzuki, E. Gomez, Q. Ji, N. Tohnai, T. Nakamura, and A. Douhal, *J. Am. Chem. Soc.*, 2019, **141**, 2111–2121.
- [S2] Y. L. Wu, N. E. Horwitz, K. S. Chen, D. A. Gomez-Gualdron, N. S. Luu, L. Ma, T. C. Wang, M. C. Hersam, J. T. Hupp, O. K. Farha, R. Q. Snurr and M. R. Wasielewski, *Nat. Chem.*, 2017, **9**, 466-472.
- [S3] Z. Wang, Y. Li, P. Liu, Q. Qi, F. Zhang, G. Lu, X. Zhao and X. Huang, *Nanoscale*, 2019, **11**, 5330-5335.
- [S4] S. Xu, G. Wang, B. P. Biswal, M. Addicoat, S. Paasch, W. Sheng, X. Zhuang, E. Brunner, T. Heine, R. Berger and X. Feng, *Angew. Chem. Int. Ed.*, 2019, **58**, 849-853.
- [S5] G. Zhao, H. Li, Z. Gao, L. Xu, Z. Mei, S. Cai, T. Liu, X. Yang, H. Guo and X. Sun, *Adv. Funct. Mater.*, 2021, **31**, 2101019.
- [S6] D.-H. Yang, Z.-Q. Yao, D. Wu, Y.-H. Zhang, Z. Zhou and X.-H. Bu, *J. Mater. Chem. A*, 2016, **4**, 18621-18627.
- [S7] G. Wang, N. Chandrasekhar, B. P. Biswal, D. Becker, S. Paasch, E. Brunner, M. Addicoat, M. Yu, R. Berger and X. Feng, *Adv. Mater.*, 2019, **31**, 1901478.
- [S8] Z. Luo, L. Liu, J. Ning, K. Lei, Y. Lu, F. Li and J. Chen, *Angew. Chem. Int. Ed.*, 2018, **57**, 9443-9446.
- [S9] V. Singh, J. Kim, B. Kang, J. Moon, S. Kim, W. Y. Kim and H. R. Byon, *Adv. Energy Mater.*, 2021, **11**, 2003735.
- [S10] S. Wang, Q. Wang, P. Shao, Y. Han, X. Gao, L. Ma, S. Yuan, X. Ma, J. Zhou, X. Feng and B. Wang, *J. Am. Chem. Soc.*, 2017, **139**, 4258-4261.